International Journal of Biological Macromolecules 124 (2019) 802–809

Contents lists available at ScienceDirect

International Journal of Biological Macromolecules

journal homepage: http://www.elsevier.com/locate/ijbiomac

Synthesis, characterization and antimicrobial activity of Schiff bases from chitosan and salicylaldehyde/TiO_2 nanocomposite membrane

A.S. Montaser [a,b,*], Ahmed.R. Wassel [c], Oqba N. Al-Shaye'a [d]

[a] Pretreatment & Finishing of Cellulose Based Textiles Department, National Research Center, Dokki, Giza 12622, Egypt
[b] Forest Biomaterial Department, College of Natural Resources, North Carolina State University, Raleigh, Campus box 8005, USA
[c] Electron Microscope & Thin Film Department, Physics Division, National Research Center, Dokki, Giza 12622, Egypt
[d] Center of Desert Studies (CDS), University of Anbar, Ramadi, Anbar, Iraq

ARTICLE INFO

Article history:
Received 24 October 2018
Received in revised form 17 November 2018
Accepted 25 November 2018
Available online 28 November 2018

Keywords:
Chitosan
Salicylaldehyde
TiO_2 NPs
Membrane
Schiff base
Antibacterial activity

ABSTRACT

Salicylaldehyde (SA) successfully used as a mono aldehyde crosslinker with chitosan forming hydrogel membrane in presence of TiO_2 NPs through casting technique. FTIR, XRD, SEM-EDX and TGA used to characterized and examining membrane physical and thermal properties. Swelling percent was evaluated for the fabricated membranes to visualize the crosslinking effect of SA Antibacterial activity evaluated using CFU methods against *S. aureus*, *P. aeruginosa*. FTIR revealed the formation of Schiff based reaction, while XRD demonstrated the presence of Titanium NPs patterns and approved bond formation between of chitosan and TiO_2 NPs. SEM-EDX approve the crosslinking and TiO_2 NPs dispersity on membrane surface. Crosslinking was enhanced using SA and TiO_2 until reaching 1 ml of SA and 0.5 mg of TiO_2 inside membrane formulation. TGA confirmed the improvement of thermal behavior in presence either crosslinking or nanometals. Mechanical properties enhanced using both crosslinker and TiO_2 nanoparticle at membrane formulation. The obtained findings validated that the nanoparticles affect strength properties while crosslinker affects plasticity. All formulated membranes showed an effective antimicrobial activity towards *S. aureus* and *P. aeruginosa* and exhibits full eradication of bacteria under investigation.

1. Introduction

Hydrogel membrane sheets are defined as water-swollen network, usually synthesized from hydrophilic polymers swelled but not dissolved [1]. Membranes produced either from natural and/or synthetic. Membranes utilizing for different applications such as electrical, food packing [2], water purification and desalination [3], medical applications [4], … etc.

However, membrane formation containing multistep (solubilization, fabrication, crosslinking and drying), Crosslinking process considered as the vital role for membrane formation, it's affecting membrane properties. Crosslinking properties exhibited via numerous ways; physical, chemical and radiation. Di-function like glutaraldehyde or monofunction like salicylaldehyde often use for membrane formation [5].

Membranes obtained from natural products as chitosan through reacting with aldehydes [6], aldehyde used in membranes formation should have better premises for safer bio-related applications. Herein, we explored the obtaining of hydrogels based on the natural products, chitosan and Salicylaldehyde, in order to provide a hydrogel appropriate for bio-medical applications, and to pave a way of chitosan crosslinking by a new friendly method.

Chitosan, as a second available polysaccharide on the earth, has a linear structure consists of [β-(1,4)-2-amino-deoxy-D-glucopyranose]. Chitosan intelligent structure possesses two active groups. Amino group located at C2 and hydroxyl group presented at C3 and C6 [7]. Chitosan through its function can be modified or grafted with another monomers. In the same time, it can form nanocomposites with nanometals. Chitosan amino group allows reacting with carbonyl or ketone groups forming Schiff bases. Schiff base compounds containing an imine group (—RCN—), are usually formed by the condensation of a primary amine with an active carbonyl [8]. Its attractiveness as analytical reagents rises from the fact that they enable simple and inexpensive determinations of various organic and inorganic substances [9].

Many scientists appeal attention to Salicylaldehyde as a safe monoaldehyde crosslinker, it's characterized with antifungal and antimycotoxiginic and chemo sensitizing properties [10]. Moreover, amine properties grant antimicrobial activity. For these reasons, its recommended to be a chitosan crosslinker [11].

Schiff base of chitosan and salicylaldehyde has been published. Further, their metal complexes with Cu, Ni and Zn have been proven [12,13].

* Corresponding author at: Pretreatment & Finishing of Cellulose Based Textiles Department, National Research Center, Dokki, Giza 12622, Egypt.
E-mail address: amontas@ncsu.edu (A.S. Montaser).

https://doi.org/10.1016/j.ijbiomac.2018.11.229
0141-8130/

Recently, nanometals used as polymer forming membranes as Titanium dioxide (TiO_2) particles, which have significant antibacterial activity and act as reinforcing compound to provide substantial mechanical strength to the scaffolds for supporting cell growth [14]. The American Food and Drug Administration has approved and recommended the use of TiO_2 in healthcare, cosmetics and food materials due to its low toxicity [15].

The composite CS/TiO_2 membrane has potential surface properties and antibacterial activities [16]. It also supports attachment, growth and proliferation of the cells, and improves tissue engineering. Besides, CS/TiO_2 composite membrane has been shown to induce re-epithelialization and promote wound healing. To the best of our mind, there are no reports dedicated to Salicylimine–chitosan membrane containing metal oxide nanoparticles like TiO_2, neither on their formation nor their properties. Thus, the current work studied and reported here reveals a novel membrane with significant mechanical properties, fast swelling, and superior antibacterial activity estimated by CFU experiment.

2. Materials and methods

2.1. Materials

Chitosan medium molecular weight 152 K, SA and TIPP (titanium isopropoxide) was purchased from Sigma-Aldrich; HCl, ethanol, water and all other chemicals are laboratory grades.

2.2. Experimental

2.2.1. Preparation of TiO_2 NPs by sol-gel technique

TiO_2 nanoparticles were synthesized via sol-gel method. Seven mL TIPP was mixed with 20 mL ethanol absolute and hydrochloric acid 0.20 mL reaching pH 8, respectively, forming ethanolic solution prepared solution aged for 24 h at 60 °C followed by drying for 24 h at 100 °C. Finally, the as-prepared powder was calcined at 500 °C for 2 h [17].

2.2.2. Synthesis of salicylamine-chitosan Schiff base

Salicylaldehyde was used without additional purification. The biopolymeric Schiff bases were synthesized by dissolving 1 g chitosan in diluted 1% acetic acid solution. Then, a desired amount of salicylaldehyde previously dissolved in 10.0 mL of ethanol was added to the chitosan solution. The reaction mixture was then let to react under the different ratios of chitosan:Salicyladehye (1:0.5), (1:1) (1:1.5) and (1:1) subsequently [18].

2.2.3. Fabrication of membrane nanocomposite

Various solutions were mixed with TiO_2 nanoparticles (0.5, 0.1 and1.5 g) suspension under vigorous stirring at 37 °C for 1 h. Solutions are casted into a Teflon molds. The mixture was kept at (70 °C) for 24 h to complete the Schiff base gelation.

2.3. Characterization

2.3.1. Attenuated total reflection (ATR-FTIR) spectroscopy

(JASCO INFRARED SYSTEM) spectroscopes equipped with an ATR were used to record and analyze the blank and modified samples. A total of 30 accumulative scans were taken per sample with a resolution of 4 cm^{-1}, in the frequency range of 4000–400 cm^{-1}, in the transmission mode.

2.3.2. X-ray diffraction

To confirm the structural properties of the prepared nanoparticles, the X-ray diffraction (XRD) was performed at room temperature using A Philips (X Pert Multi-Purpose diffraction) operated at 40 kV/30 mA.

2.3.3. Scanning electron microscope (SEM-EDX)

Microscopic investigations on membrane samples were carried out using a Philips XL30 scanning electron microscope (SEM) equipped with a LaB6 electron gun and a Philips-EDAX/DX4 energy-dispersive spectroscope (EDS). Images were taken at different magnifications using secondary electrons (SE) in accordance with the clarity of the images. Membrane samples were fixed with carbon glue and metalized by gold vapor deposition to record images.

2.3.4. Transmission electron microscope (TEM)

The morphology, size and shape of the synthesized TiO_2 nanoparticles were imaged by means of a JEOL-TEM-1200 Electron Microscope. TiO_2 NPs powder dispersed in deionized water by ultrasonic vibration. Which was observed by TEM placing a drop onto a carbon-coated copper grid (model: JEOL JEM 1011) operating at 80 kV, using a CCD camera (Hitachi H-7600, AMT V600).

2.3.5. Mechanical properties

Membrane samples were tested for the change in their tensile and elongation properties. The breaking load of the samples was determined by the strip method on tensile tester instrument (ASANO Machine MFG.CO, DSAKA, No.6202, Japan) [19].

2.3.6. Thermal gravimetric analysis (TGA)

Thermal gravimetric analysis (TGA) Thermal gravimetric analysis TGA was carried out on Perkin–Elmer Pyris TGA in N_2 atmosphere, temperature range of 40–600 °C, and heating rate of 10 °C/min.

2.3.7. Antibacterial activity

Determination of antibacterial activity was evaluated by measuring the colony forming units CFU. The bacteria from the stock culture, *Staphylococcus aureus* and *Pseudomonas aeruginosa*, were inoculated into a freshly prepared liquid nutrient broth containing (g/l): peptone (5); beef extract (3) at pH 6.8, and incubated for 24 h. Samples, 0.25 g of membrane samples were added to the inoculated flasks, containing 10 ml nutrient broth, leaving the control (untreated sample). After 24 h incubation at 37 °C, a serial dilution from each sample-containing culture and the control has been done (10^{-1}–10^{-9}). The microbial inhibition was determined by counting the colony forming units (CFU) by inoculating petri-dishes containing solidified nutrient agar medium with 100 μl from each dilution and calculating the reduction growth rate (R) for treated samples in relation to control (untreated) according to the equation

$$R\ (\%) = B–A/B \times 100$$

where A is CFU/ml for treated sample after 16 h incubation and B is CFU/ml for untreated sample after the same period of incubation time [20].

3. Results and discussions

3.1. TiO_2 nanoparticles formation and characterization

The crystal structures of after-calcined TiO_2 powder was examined by X-ray diffraction analysis and the corresponding results are illustrated in Fig. 1a. It can be seen that the as-synthesized pure TiO_2 powder showed that all peaks corresponded to anatase TiO_2 phase. It's obvious scattering angles 2θ of 23°, 25.3°, 38.3°, 48°, 54°, and 62° pointing to anatase faces (101), (004), (200), (105) and (204). The crystallite size (d) of crystalline anatase phase was estimated by Scherer's equation as follows

$$d = 0.9\lambda/\beta\ \cos\theta$$

Note that d is the crystallite size, K is the shape factor (0.9), λ is the X-ray wave length of Cu K_α (0.154 nm), β is the full-width at half

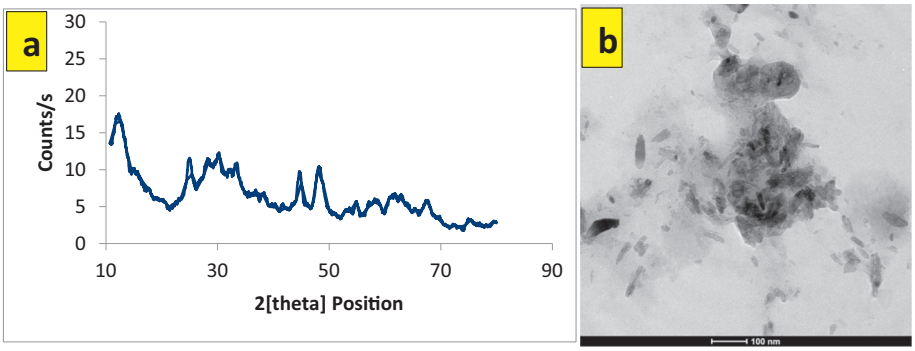

Fig. 1. TiO_2 NPs characterization; a) XRD and b) SEM.

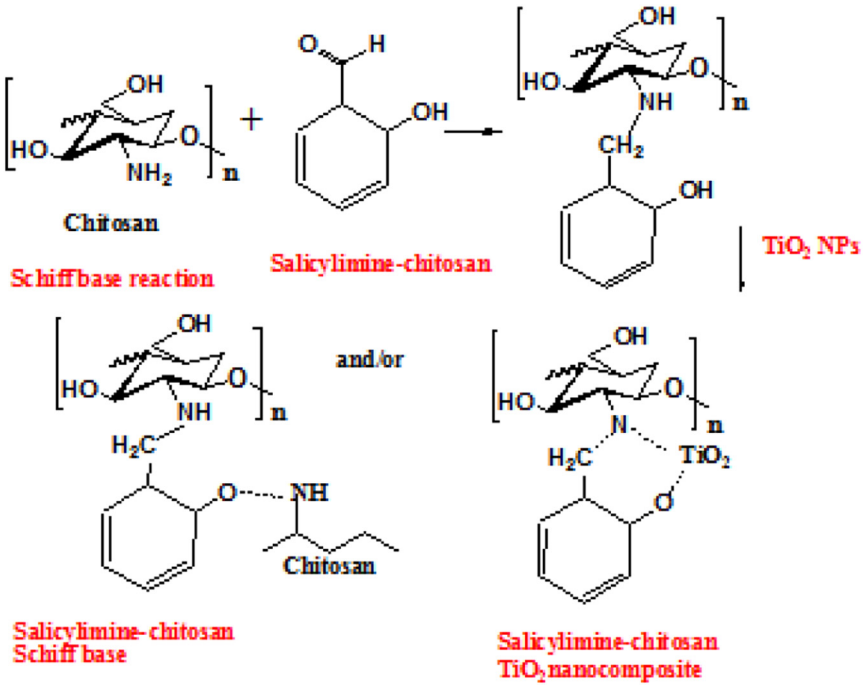

Scheme 1. Schiff base reaction and of chitosan and salicylaldehyde/TiO_2 nanocomposite.

maximum (FWHM) and θ is the diffraction angle of the major peak of anatase phase located at 2θ = 25.4°. The average crystallite size of TiO_2 is d = 11.7 nm. TEM micrographs of TiO_2 nanoparticles are presented in Fig. 1a. The micrographs of both samples showed that the particle sizes of TiO_2 sample is in nano-scale. The results of particle sizes from TEM are consistent with the observation from XRD.

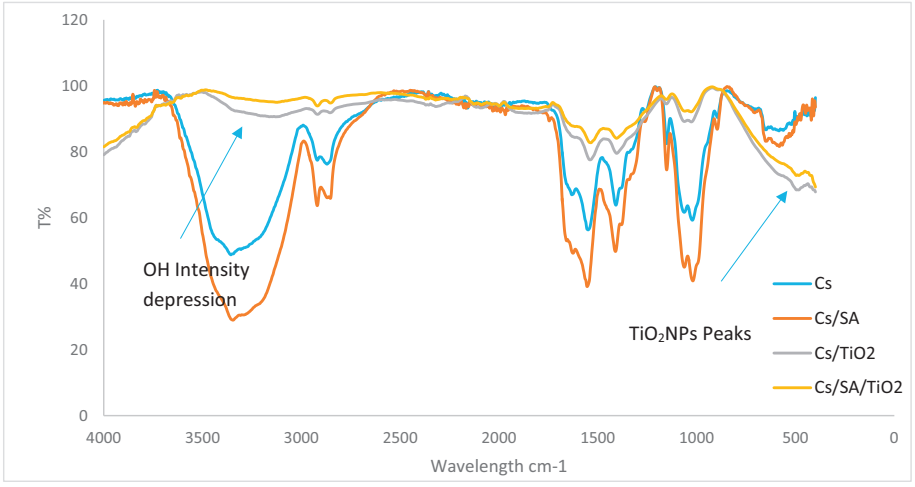

Fig. 2. ATR-FTIR of the prepared membranes.

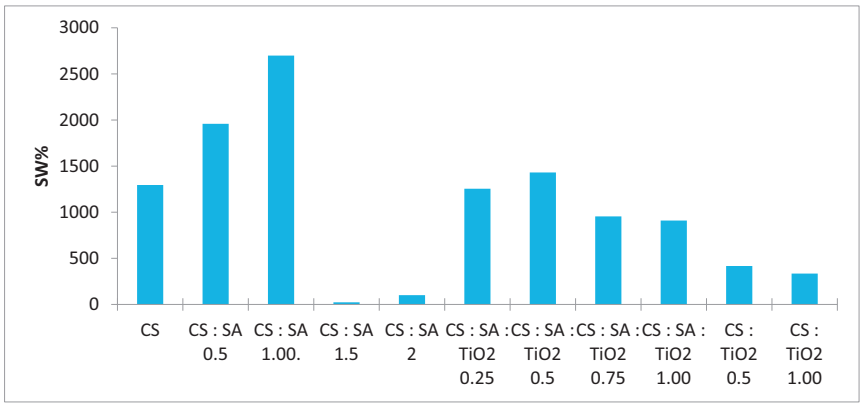

Fig. 3. Swelling percent of the prepared membranes.

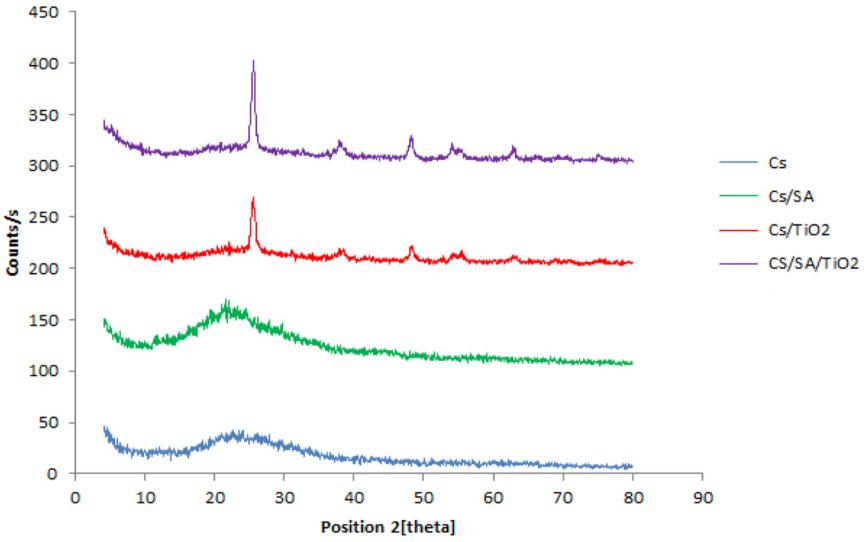

Fig. 4. XRD of prepared membranes: 1) Cs, 2) Cs: SA, 3) Cs/TiO_2 and 4) Cs: SA/TiO_2 nanocomposites.

3.2. Attenuated total reflectance (ATR)

Chitosan and salicylaldehyde reacted via Schiff base as demonstrate in Scheme 1, chitosan amino group and aldehydic group of SA reacted via nucleophilic attack forming amid group, while the hydroxyl group of SA can react with another amino group of another chitosan chain via electrostatic interaction. In case of TiO_2 presence, the reaction tends to react with TiO_2NPs through metal complex theory. Cs-SA Schiff base can form metal complex with TiO_2NPs through coordination bond, transition metals has a vacant orbitals which assist electron donating groups like amino chitosan and hydroxyl of SA to form this bond. The comparative structural conformation of Cs and Cs/TiO_2 nanocomposite membranes were determined from the characteristic transmittance peaks of the infrared spectrum (Fig. 2). The spectrum of unconjugated CS exhibited a band at 3370 cm^{-1} that was due to the symmetrical stretching vibrations of OH and NH groups. The peak at 2875 cm^{-1}

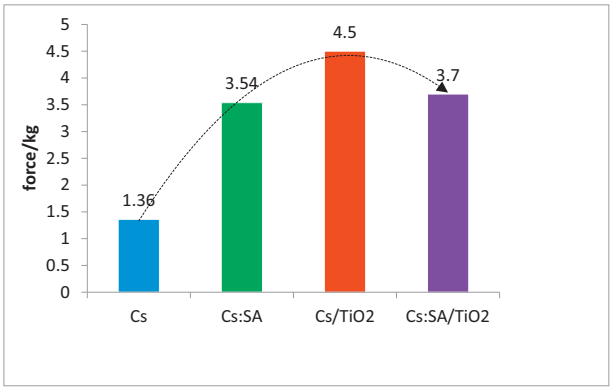

Fig. 5. Tensile strength of 1) Cs, 2) Cs: SA, 3) Cs/TiO_2 and 4) Cs: SA/TiO_2 membranes nanocomposite.

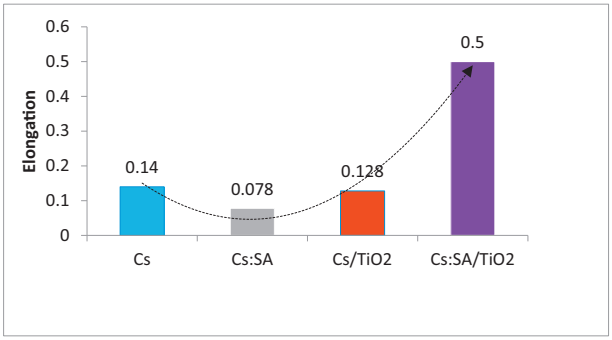

Fig. 6. Elongation percent of 1) Cs, 2) Cs: SA, 3) Cs/TiO_2 and 4) Cs: SA/TiO_2 membranes nanocomposite.

was attributed to the asymmetric stretching of CH group in the polymer. However, the peaks attributed to CH_2 asymmetric vibration could easily be seen at 1429 and 1319 cm^{-1} in all the spectrums. The ATR-FTIR spectral absorption bands of 1660 cm^{-1} and 1577 cm^{-1} correspond to the vibrational frequencies of chitosan structure that was reported as amides I (C O stretching and N H deformation). The special peak of (1–4) glycoside bond in polysaccharide unit an stretching vibration of C—O—C in glucose circle were assigned to the peaks at 1157 $cm^{-1}$and 1037 cm^{-1} respectively. The ATR spectral bands of stretching vibration between 3000 and 3750 cm^{-1} were attributed to hydroxyl group (OH) and the NH group in case CS/SA, CS/TiO_2 and Cs/SA/TiO_2 composite membranes (Fig. 2) with respect to unconjugated chitosan. Moreover, the composite membrane containing TiO_2 NPs are characteristic O—Ti—O bands at 400–700 cm^{-1} that were ascribed to the immobilization of TiO_2 into the CS matrix.

The ATR data also revealed that the bands corresponding to hydroxyl, amino and amide groups in the spectrum of composite membrane were shifted as compared to the unconjugated CS. These shifting in ATR bands further confirmed the interaction between CS and SA and turned to be more intense. Salicylaldehyde as a monoaldehyde can react directly with amino group present on chitosan chain forming Schiff base and repulsion, while the intensity of OH group at the produced molecule increases forming hydrogen bond between hydroxyl group present at salicylaldehyde and OH present at chitosan, which affect positively on the intensity peak of hydroxyl group. On the other hand, membrane composite decreases OH peak intensity. The finding of our study was found in consistent with the observation of Halloran and Shim [21]. The original peaks of ATR represent chitosan from OH, NH and CH_2 and acetyl groups come to decrease at intensity in presence of TiO_2, it may be attributed to complexation between these functions and titanium atom, as known Ti a lanthanide metal have a vacant orbital, hydrogen atom from OH group of the glycoside ring can make a coordination bond with titanium and forming complex. Also this complex has a good chance to be exhibited absence of crosslinking.

3.3. Swelling properties

Swelling percent reflect the ability of membrane to retain water molecule inside its network, Synthesis of membrane with different concentrations of crosslinker was carried out Fig. 3 illustrates the swelling value against membranes composition. It's obvious that swelling percent increases with crosslinker density reaching 1 ml of SA counted 2698% in comparison with chitosan membrane 1500%, then swelling decline with increasing SA percent. As known, crosslinker assists pores boundaries which reflecting positively on swelling percent. These swellings reflect to the elasticity of membrane pore walls, therefore, it can absorb water molecule inside. Similarly to the previous mechanism, TiO_2 nanoparticles crosslinked via electrostatic and covalent pounds between Titanium dioxide nanoparticles and chitosan. However, the low percent of TiO_2 showed strong depression of swelling data nearly 500%. The effect of combination between the best composition between crosslinking and chitosan (Cs: SA 1) and different percent of TiO_2 was evaluated. The swelling percent increases with the following rational formulation (Cs: SA_1: TiO_2 0.5).

3.4. X ray diffraction (XRD)

To analyze the crystalline structure of the prepared membranes CS and CS/SA, Cs/TiO_2 and Cs/SA/TiO_2 nanocomposite membranes, XRD analysis has been accomplished (Fig. 4). The XRD of chitosan clearly appears at Fig. 4a. The significant broad band of glycoside represents at 28°, while the crosslinked membranes containing SA did not showed any significant change (Fig. 4-2), this means that there is no effect of chitosan crystallinity. While, XRD patterns (Fig. 4c) revealed the intense diffraction peaks at 25.4°, 37.9°, 48.2°, 54.02°, and 55.22° for TiO_2 at CS/TiO_2 composite membranes. It's combined with depression and deformation of chitosan peak which appears at the same place of anatase TiO_2 [22]. The depression of chitosan intensity means deformation of chitosan crystallinity, it's as a reason of dramatically interfered with the ordered packing of polymer chains by both steric effect and

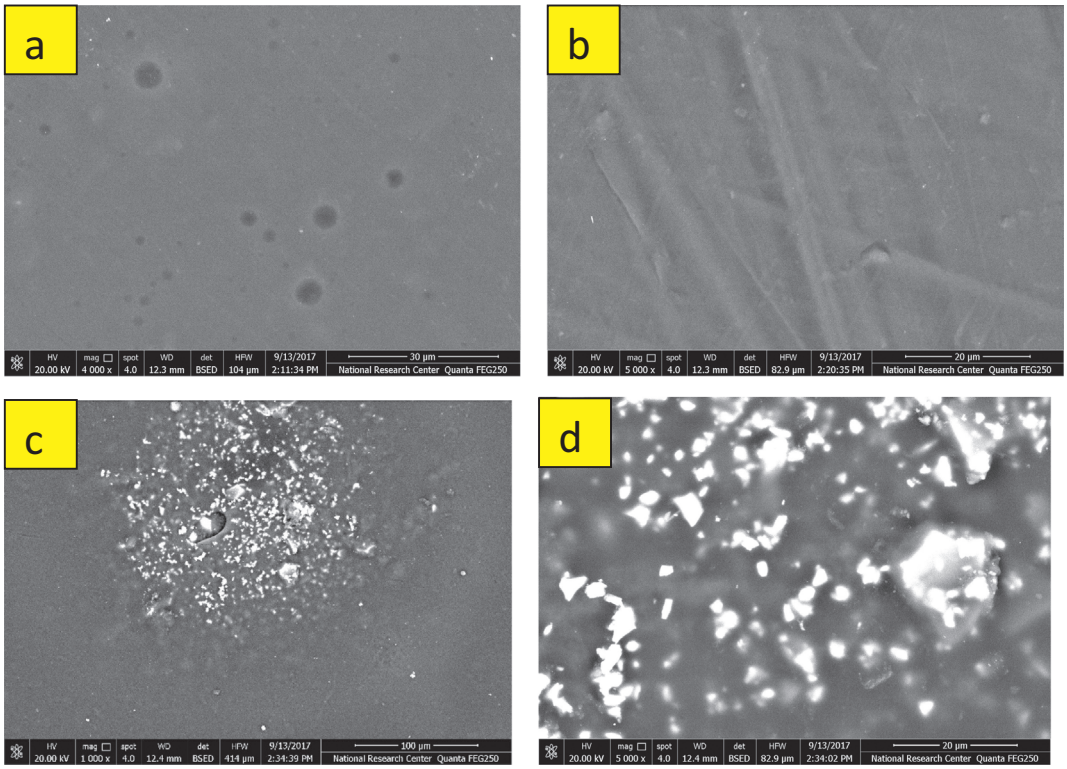

Fig. 7. SEM of: 1) Cs, 2) Cs: SA, 3) Cs/TiO_2 and 4) Cs: SA/TiO_2 membranes nanocomposite.

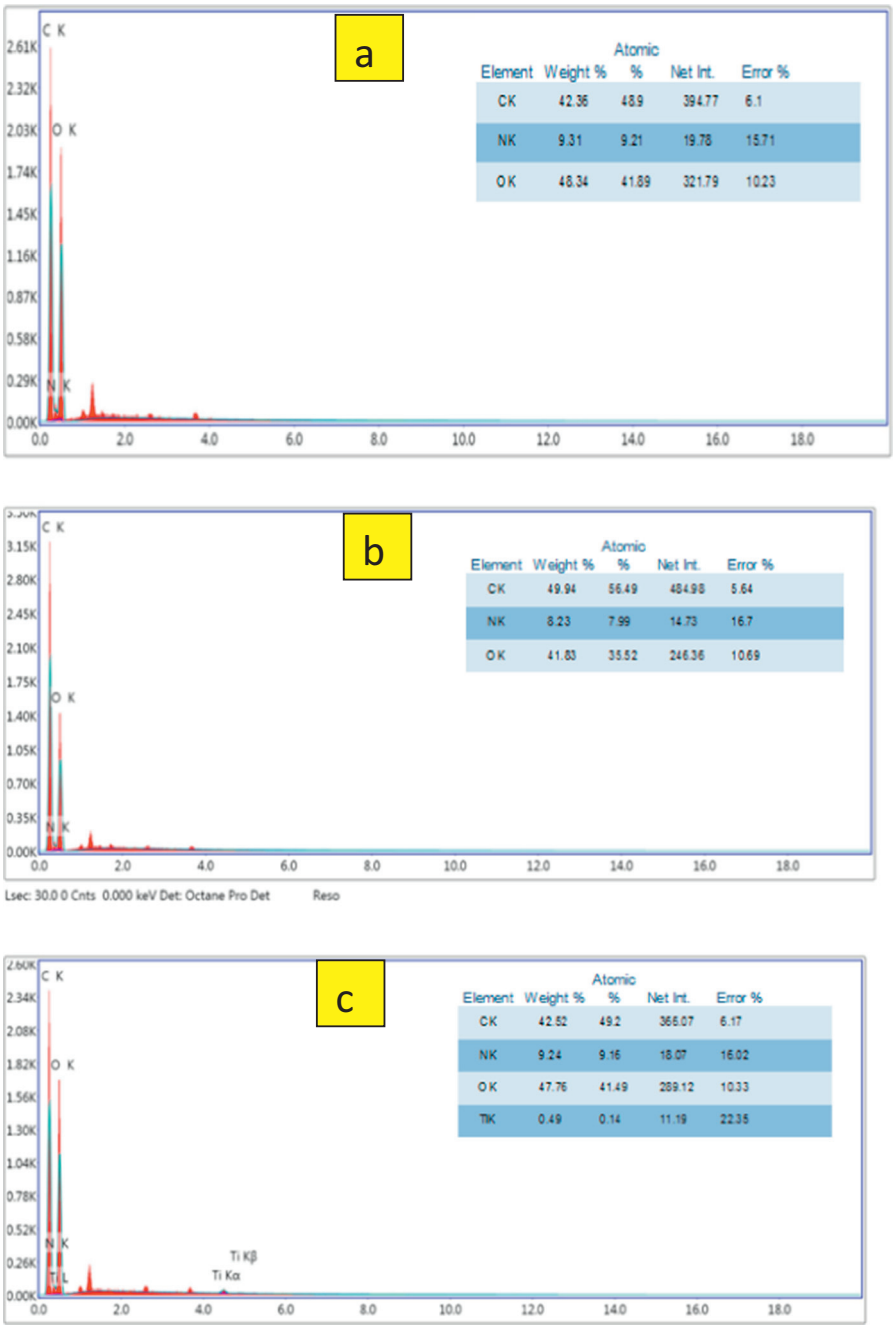

Fig. 8. EDX patterns for the prepared membranes.

hydrogen bonds between CS and TiO_2, leading to the decrease in CS crystallinity. The presence of SA as crosslinker at XRD pattern (Fig. 4d) showed positively on TiO_2 crystallinity appears at high intensity of the peaks when compared with Cs/TiO_2 membranes. This may be attributed to present free TiO_2 as a result of Schiff base crosslinking between chitosan and salicylaldehyde.

3.5. Mechanical measurements

The mechanical properties of the prepared membranes were evaluated through tensile strength and elongation percent analysis. Tensile strength (TS), Elongation modulus (EM) values of Cs and Cs blend membranes containing different TiO_2 NPs and SA are presented in Fig. 5. The presence of either SA crosslinker and/or TiO_2 increase tensile strength compared with chitosan membrane itself. The addition of TiO_2 NPs

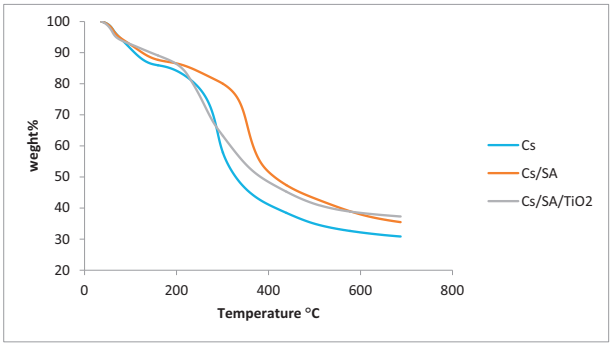

Fig. 9. Thermal gravimetric analysis (TGA) of 1) Cs, 2) Cs/SA and 3) Cs/SA/TiO_2 membranes nanocomposite.

into CS-matrix acts as mechanical reinforcement leading to significant increase of TS. Whilst, combination of SA/TiO_2 decrements tensile values. It is as a reason of free deposited TiO_2 inside the membrane as result of chitosan salicylaldehyde crosslinking. Moreover, the blending of TiO_2 to CS also changed the rigidity of the composite membranes and consequently resulted in decrease of the Eb value (Fig. 6). The data declare the incorporation of TiO_2 NPs increases rigidity during the time SA crosslinker increases plasticity. The mechanical strength enhancement would be utilized at medical applications, food backing and wound healing.

3.6. Scanning electron microscope (SEM)

The surface morphology of pure CS, CS/TiO_2, CS/SA and CS/SA/TiO_2 membranes nanocomposite were observed with SEM (Fig. 7). There are smooth waves like structure found on the surface of the pure CS membrane (Fig. 7a). While, the addition of SA crosslinker (Fig. 7b) to chitosan membrane formulation showed as straight threads inside the scanned membrane which reflect the crosslinking process. The addition of TiO_2 NPs to the CS matrix made the surface of composite membrane unsmooth with many minute granules (Fig. 7c) and enhanced forming pores. In the same time, the incorporation of TiO_2 /SA to CS membrane showed irregular shape of membrane with deposited TiO_2 NPs (Fig. 7d), the results demonstrate that TiO_2 NPs come to deposit or phase separation on the surface because chitosan tend to react with SA than forming covalently bond with TiO_2 NPs [23]. These images correlate with XRD results which demonstrate higher intensity of TiO_2 when combined with SA and chitosan. Fig. 8 shows The Energy Dispersive Analysis X-ray data reveal the incorporation of TiO_2 inside the prepared membranes.

3.7. Thermal gravimetric analysis (TGA)

The thermal properties of the prepared three components Cs, Cs/SA and Cs/SA/TiO_2 membrane nanocomposite were studied; TGA curves obtained are illustrated in Fig. 9. Shows there were three distinct weight-loss stages in the TG curve of pure CS membrane. The first was from room temperature to 110 °C, which can be assigned to the evaporation of residual solvents, mainly H_2O. At the second stage, the weight-loss region of 110–350 °C corresponded to the decomposition of CS main chain. The third stage happened between 350 and 800 °C, which was associated with further decomposition of CS molecules. In the case of Cs/SA it's more broad than the Cs decomposition peak, and its characterized with high ash. This rather expected, thermal stability of CS/SA membrane enhanced as a reason of Schiff base reaction. On the other hand, CS/SA/TiO_2 membrane nanocomposite showed a different characteristic peak which approves the theory of alternation or deformation of chitosan crystallinity forming new bonds with its chains. Titanium bonds might be formed via two ways: one occurred between —OH groups in different titanium atoms, and the other occurred

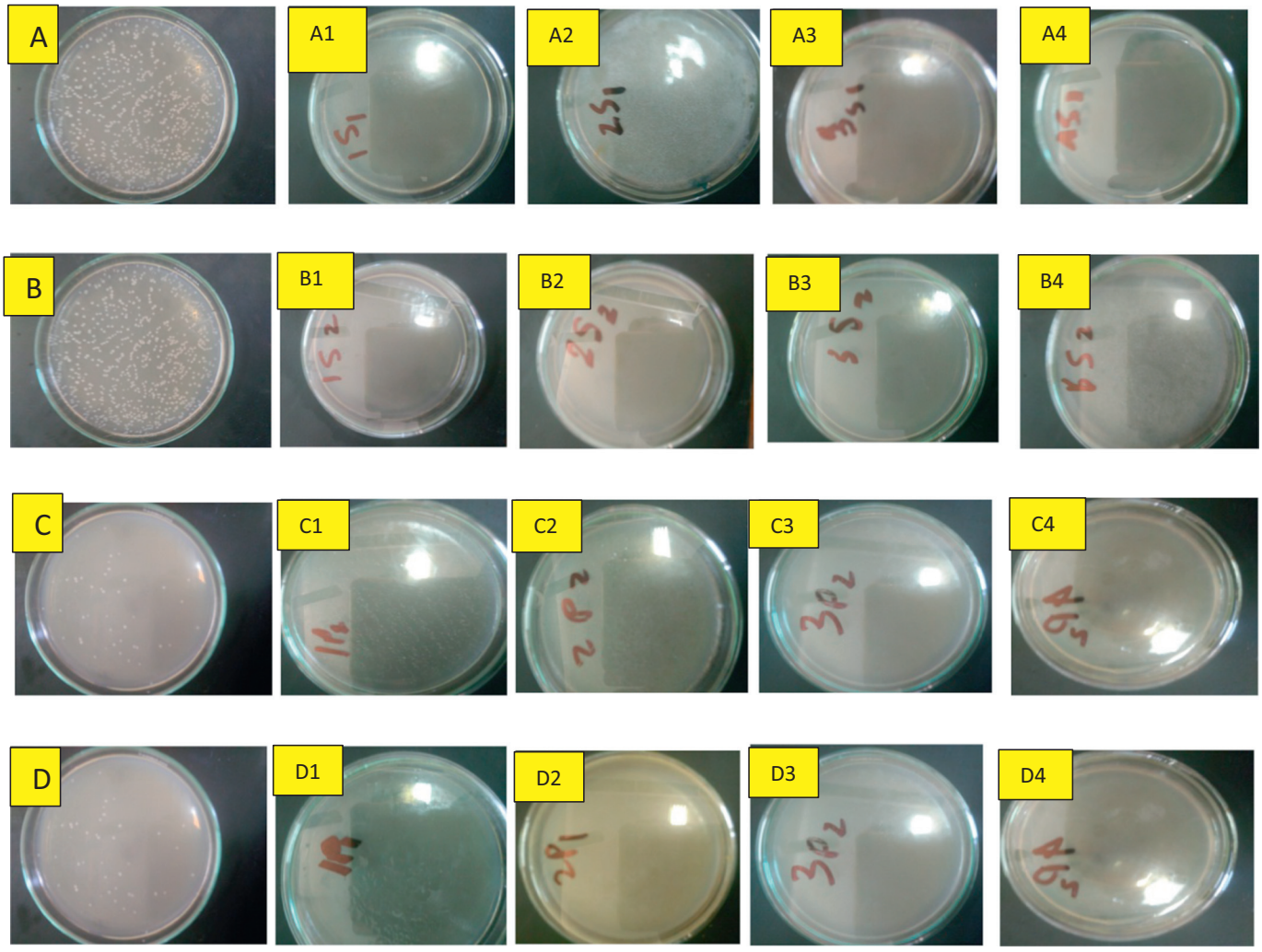

Fig. 10. Antibacterial activities using CFU method against A) *S. aureus* sample concentration 0.25 mg/100 ml, B) *S. aureus* sample concentration 0.5 mg/100 ml, C) *P. aeruginosa* sample concentration 0.25 mg/100 ml and D) *P. aeruginosa* sample concentration 0.5 mg/100 ml. Where 1) Cs, 2) Cs: SA, 3) Cs/TiO_2 and 4) Cs: SA/TiO_2 membranes nanocomposite.

between —OH groups in titanium and —OH groups in CS chains. In addition, —NH_2 groups in CS chains were protonated to form —NH_3^+, which could subsequently connect with Ti—OH groups through hydrogen bonds [24], improves thermal stability to the CS/SA/TiO_2 membrane nanocomposite; a point which verifying that introduction of TiO_2 NPs into the composite enhances firmly thermal property.

3.8. Antibacterial activity

The antibacterial activity was evaluated towards (*S. aureus* and *P. aeruginosa*), Gram-positive and Gram-negative bacteria, which commonly found on skin and in wound infection. CFU method used to evaluate its antibacterial activity in comparison with bacterial cultural growth at the same conditions. The *S. aureus* and *P. aeruginosa* exposed to membrane composition with two concentrations (0.25 and 0.5 g/100 ml). CFU results of the membranes under test CS, CS: SA, CS/TiO_2 and Cs: SA/TiO_2 membranes is given in (Fig. 10) shows complete eradication to the two types of bacteria. It's needn't to say that the cationic amino group exhibited on chitosan chains has a superior antimicrobial activity. Three antibacterial mechanisms have been proposed: i) the ionic surface interaction resulting in wall cell leakage; ii) the inhibition of the mRNA and protein synthesis via the penetration of chitosan into the nuclei of the microorganisms; and iii) the formation of an external barrier, chelating metals and provoking the suppression of essential nutrients to microbial growth. It is likely that all events occur simultaneously but at different intensities [25,26]. In addition, TiO_2 catalytic nanometals, known by antimicrobial and catalytic activity. The synergistic effect of the combination didn't appear clearly because of the high content of each composition. Also, the aldehyde group present at SA crosslinker may act as antibacterial inhibitor. These results confirm the potency of the prepared membranes to be used in medical field's especially antibacterial membranes.

4. Conclusion

Salicylimine-chitosan/TiO_2 nanocomposite has been prepared and fully characterized through instrumental tools, TiO_2 NPs prepared via sol-gel technique confirmed through XRD and TEM. The interaction between SA and/or TiO_2 NPs clearly appears at ATR-FTIR through change at OH intensity and new exhibited peaks. SEM-EDX screening the morphology of the prepared membrane and Titanium nanoparticles surface distribution. The presence of SA with TiO_2 improves the physical properties, especially thermal analysis and mechanical properties chiefly elongation percent. All prepared membranes expressed antibacterial activity through CFU method, and demonstrated fully bacterial eradication. The prepared membranes are qualified to be used as antibacterial membrane especially at food backing and wound dressing applications.

References

[1] A.M. Abdel-Mohsen, A.S. Aly, R. Hrdina, A.S. Montaser, A. Hebeish, Eco-synthesis of PVA/chitosan hydrogels for biomedical application, J. Polym. Environ. (2011) https://doi.org/10.1007/s10924-011-0334-0.

[2] K. Gładyszewski, M. Skiborowski, Additive manufacturing of packings for rotating packed beds, Chem. Eng. Process. Process Intensif. 127 (2018) 1–9, https://doi.org/10.1016/j.cep.2018.02.024.

[3] Energy use for membrane seawater desalination – current status and trends, Desalination 431 (2018) 2–14.

[4] F. Galiano, K. Briceño, T. Marino, A. Molino, K.V. Christensen, A. Figoli, Advances in biopolymer-based membrane preparation and applications, J. Membr. Sci. 564 (2018) 562–586, https://doi.org/10.1016/j.memsci.2018.07.059.

[5] Y. Jia, J. Li, Molecular assembly of Schiff base interactions: construction and application, Chem. Rev. 115 (2015) 1597–1621, https://doi.org/10.1021/cr400559g.

[6] V.B. Gavalyan, Synthesis and characterization of new chitosan-based Schiff base compounds, Carbohydr. Polym. 145 (2016) 37–47, https://doi.org/10.1016/j.carbpol.2016.02.076.

[7] A.A. Hebeish, M.A. Ramadan, A.S. Montaser, A.M. Farag, Preparation, characterization and antibacterial activity of chitosan-g-poly acrylonitrile/silver nanocomposite, Int. J. Biol. Macromol. 68 (2014) 178–184, https://doi.org/10.1016/j.ijbiomac.2014.04.028.

[8] S.M. Anush, B. Vishalakshi, B. Kalluraya, N. Manju, Synthesis of pyrazole-based Schiff bases of chitosan: evaluation of antimicrobial activity, Int. J. Biol. Macromol. 119 (2018) 446–452, https://doi.org/10.1016/j.ijbiomac.2018.07.129.

[9] M. Sahin, N. Kocak, G. Arslan, H.I. Ucan, Synthesis of crosslinked chitosan with epichlorohydrin possessing two novel polymeric ligands and its use in metal removal, J. Inorg. Organomet. Polym. Mater. 21 (2011) 69–80, https://doi.org/10.1007/s10904-010-9421-2.

[10] J.E. dos Santos, E.R. Dockal, É.T.G. Cavalheiro, Synthesis and characterization of Schiff bases from chitosan and salicylaldehyde derivatives, Carbohydr. Polym. 60 (2005) 277–282, https://doi.org/10.1016/j.carbpol.2004.12.008.

[11] M.-M. Iftime, S. Morariu, L. Marin, Salicyl-imine-chitosan hydrogels: supramolecular architecturing as a crosslinking method toward multifunctional hydrogels, Carbohydr. Polym. 165 (2017) 39–50, https://doi.org/10.1016/j.carbpol.2017.02.027.

[12] H.F.G. Barbosa, É.T.G. Cavalheiro, The influence of reaction parameters on complexation of Zn(II) complexes with biopolymeric Schiff bases prepared from chitosan and salicylaldehyde, Int. J. Biol. Macromol. (2018)https://doi.org/10.1016/j.ijbiomac.2018.10.113.

[13] E.L. de Araújo, H.F.G. Barbosa, E.R. Dockal, É.T.G. Cavalheiro, Synthesis, characterization and biological activity of Cu(II), Ni(II) and Zn(II) complexes of biopolymeric Schiff bases of salicylaldehydes and chitosan, Int. J. Biol. Macromol. 95 (2017) 168–176, https://doi.org/10.1016/j.ijbiomac.2016.10.109.

[14] K.T. Karthikeyan, A. Nithya, K. Jothivenkatachalam, Photocatalytic and antimicrobial activities of chitosan-TiO_2 nanocomposite, Int. J. Biol. Macromol. 104 ((2017) 1762–1773, https://doi.org/10.1016/j.ijbiomac.2017.03.121.

[15] Z. Zhu, H. Cai, D.-W. Sun, Titanium dioxide (TiO_2) photocatalysis technology for nonthermal inactivation of microorganisms in foods, Trends Food Sci. Technol. 75 (2018) 23–35, https://doi.org/10.1016/j.tifs.2018.02.018.

[16] X. Zhang, G. Xiao, Y. Wang, Y. Zhao, H. Su, T. Tan, Preparation of chitosan-TiO_2 composite film with efficient antimicrobial activities under visible light for food packaging applications, Carbohydr. Polym. 169 (2017) 101–107, https://doi.org/10.1016/j.carbpol.2017.03.073.

[17] S. Mahshid, M. Askari, M.S. Ghamsari, N. Afshar, S. Lahuti, Mixed-phase TiO_2 nanoparticles preparation using sol–gel method, J. Alloys Compd. 478 (2009) 586–589, https://doi.org/10.1016/j.jallcom.2008.11.094.

[18] L.S. Guinesi, É.T.G. Cavalheiro, Influence of some reactional parameters on the substitution degree of biopolymeric Schiff bases prepared from chitosan and salicylaldehyde, Carbohydr. Polym. 65 (2006) 557–561, https://doi.org/10.1016/j.carbpol.2006.01.030.

[19] J. Li, W. Zhou, S. Fan, Z. Xiao, Y. Liu, J. Liu, B. Qiu, Y. Wang, Bioethanol production in vacuum membrane distillation bioreactor by permeate fractional condensation and mechanical vapor compression with polytetrafluoroethylene (PTFE) membrane, Bioresour. Technol. 268 (2018) 708–714, https://doi.org/10.1016/j.biortech.2018.08.055.

[20] M.S. Abdel-Aziz, A.M. Hezma, Spectroscopic and antibacterial evaluation of nanohydroxapatite polyvinyl alcohol biocomposite doped with microbial-synthesized nanogold for biomedical applications, Polym.-Plast. Technol. Eng. 52 (2013) 1503–1509, https://doi.org/10.1080/03602559.2013.820754.

[21] Y. Haldorai, J.-J. Shim, Novel chitosan-TiO_2 nanohybrid: preparation, characterization, antibacterial, and photocatalytic properties, Polym. Compos. 35 (n.d.) 327–333. doi:https://doi.org/10.1002/pc.22665.

[22] R. Li, K. Nie, W. Pang, Q. Zhu, Morphology and properties of organic–inorganic hybrid materials involving TiO_2 and poly(ϵ-caprolactone), a biodegradable aliphatic polyester, J. Biomed. Mater. Res., Part A 83A (n.d.) 114–122. doi:https://doi.org/10.1002/jbm.a.31224.

[23] D. Yang, J. Li, Z. Jiang, L. Lu, X. Chen, Chitosan/TiO_2 nanocomposite pervaporation membranes for ethanol dehydration, Chem. Eng. Sci. 64 (2009) 3130–3137, https://doi.org/10.1016/j.ces.2009.03.042.

[24] N. Kahya, S. Bener, H. Kaygusuz, G.A. Evingür, F.B. Erim, Adsorptive removal kinetics of anionic dye onto chitosan films doped with graphene oxide: an in situ fluorescence monitoring, Chem. Eng. Commun. 205 (2018) 881–887, https://doi.org/10.1080/00986445.2017.1423064.

[25] M. Kong, X.G. Chen, K. Xing, H.J. Park, Antimicrobial properties of chitosan and mode of action: a state of the art review, Int. J. Food Microbiol. 144 (2010) 51–63, https://doi.org/10.1016/j.ijfoodmicro.2010.09.012.

[26] B. Li, Y. Zhang, Y. Yang, W. Qiu, X. Wang, B. Liu, Y. Wang, G. Sun, Synthesis, characterization, and antibacterial activity of chitosan/TiO_2 nanocomposite against *Xanthomonas oryzae* pv. *oryzae*, Carbohydr. Polym. 152 (2016) 825–831, https://doi.org/10.1016/j.carbpol.2016.07.070.